Conceptual Electromagnetic and Mechanical Design of a Cosθ Dipole for the Muon Collider Study

Francesco Mariani, Luca Alfonso, Andrea Bersani, Luca Bottura, Barbara Caiffi, Stefania Farinon, Samuele Mariotto, Daniel Novelli, Alessandra Pampaloni, Tiina Salmi, Stefano Sorti, and Lucio Rossi, *Fellow, IEEE*

***Abstract*—Within the framework of the International Muon Collider Collaboration (IMCC), researchers are involved in a feasibility study to develop high-temperature superconducting (HTS) magnets for a 10 km collider ring, designed to reach a 10 TeV Center-of-Mass (CoM) energy.Due to the short lifetime of muons of only 2.2 μs, the machine must minimize their acceleration time, allowing them to collide before the decay. To optimize the machine cost and maximize the collider luminosity, the superconducting dipoles of the collider ring must be compact and generate high steady-state magnetic fields. In addition, they must feature large apertures for the insertion of a shielding structure needed to preserve the superconducting coils from muon decay products. These demanding specifications pose significant technological challenges for the design of the dipole magnets, both in terms of physics and engineering. In this contribution, we give an overview of the conceptual 2D electromagnetic design of the main collider dipoles, followed by a preliminary mechanical analysis for a first estimation of stresses due to the Lorentz forces. Since the coil design is based on REBCO tapes - whose magnetization effects must be taken into account - an analytical code was written in MATLAB to evaluate the magnet performances considering non-uniform current distribution according to the Brandt model.A validation study of the code by comparing its results with finite element method (FEM) simulations is also presented. In this comparison, the computational time of the analytical and numerical approaches will also be pointed out to better appreciate the importance of the work done in developing the new tool.**

***Index Terms*—2G HTS conductors, accelerator dipoles, magnetic field effects, magnetization processes, modeling.**

Received 28 July 2025; revised 2 October 2025; accepted 31 October 2025. Date of publication 10 November 2025; date of current version 25 November 2025. This work was supported by NextGeneration EU- Italian National Recovery and Resilience Plan Mission 4 - Component 2 - Investment 3.1. - Project name: IRIS under Grant CUP: I43C21000230006. *(Corresponding author: Francesco Mariani.)*

Francesco Mariani is with the Sapienza University of Rome, 00185 Rome, Italy, and also with the Laboratory of Acceleration and Applied Superconductivity, INFN - Milano, 20054 Milan, Italy (e-mail: francesco.mariani@mi.infn.it, fr.mariani@uniroma1.it).

Luca Alfonso, Andrea Bersani, Barbara Caiffi, and Stefania Farinon are with the National Institute for Nuclear Physics (INFN-Genova), 16146 Genoa, Italy.

Luca Bottura is with the European Organization for Nuclear Research (CERN), 1211 Geneva, Switzerland.

Samuele Mariotto, Stefano Sorti, and Lucio Rossi are with the Laboratory of Acceleration and Applied Superconductivity, INFN-Milano, 20054 Milan, Italy, and also with the Department of Physics, University of Milan, 20133 Milan, Italy.

Daniel Novelli and Alessandra Pampaloni are with the Sapienza University of Rome, 00185 Rome, Italy, and also with the National Institute for Nuclear Physics (INFN-Genova), 16146 Genoa, Italy.

Tiina Salmi is with the Tampere University, 33720 Tampere, Finland.

Color versions of one or more figures in this article are available at https://doi.org/10.1109/TASC.2025.3630165.

Digital Object Identifier 10.1109/TASC.2025.3630165

I. Introduction

THE International Muon Collider Collaboration[1], [2] (IMCC) is focused on investigating the feasibility of a 10 km long Muon Collider accelerator machine reaching 10 TeV Center-of-Mass energy. Differently from protons, muons are elementary particles, so their collision energy is entirely used in particle interaction studies[3]. Also, muons, being 200 times heavier than electrons, have 10^9 times lower synchrotron radiation losses[4]. Thanks to these two factors, the muon colliders can aim to state-of-the-art performance in both precision measurements and discovery physics within a remarkably compact design[5], [6]. To build a multi-TeV Muon Collider, high-field superconducting magnets are essential[7], [8]. This paper presents an updated electromagnetic design of the 16 T cosθ collider ring dipoles[9], [10] based on HTS technology. The magnets must feature a 140 mm coil aperture for the insertion of a tungsten shielding protecting the superconductor from the muon decay products. Screening currents induced by external fields significantly affect coil behavior. While finite element method (FEM) tools can achieve high accuracy accounting for this phenomenon, their computational cost is incompatible with iterative optimization. To address this, an analytical MATLAB[11] code based on the Brandt model[12] was developed to efficiently compute non-uniform screening currents. The paper includes six sections: design requirements, an overview of the Brandt analytical model and a COMSOL-based[13] T-A formulation[14], electromagnetic results for uniform and non-uniform current, a preliminary mechanical analysis, a summary of quench protection findings, and a cost estimation model.

II. Conductor and Magnet Design

Analytical studies indicate that a 16 T dipole with a coil aperture of 140 mm approaches the limits of what Nb_3Sn technology can achieve[15], [16]. Hence, high temperature superconducting (HTS) technology is being considered for the dipole magnet design of both the accelerator[17] and collider rings. Using HTS allows operation up to 20 K instead of 1.9 K, cutting cryogenic costs by a factor of ten[18]. The cable from the preliminary study[19] was updated by considering the same of the block coil design[20], [21] and compatible with a no-graded coil layout. The cable consists of two identical subunits formed by two stacked Fujikura REBCO tapes (FESC-SCH12)[22] and a stainless steel layer.

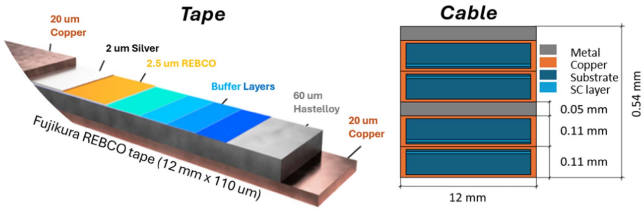

Fig. 1. Tape composition rendering (left). Cable structure (right): in dark gray the stainless steel stabilizer layer.

TABLE I
MAGNET PARAMETERS

Design parameters	Value
Coil aperture	140 mm
Central field	16 T
Peak field	18.1 T
Current	3663 A
Engineering current density	565 A/mm^2
Copper current density	1897 A/mm^2
Operating temperature	20 K
Temperature margin	2.5 K
Total inductance	0.53 H/m
Total stored energy	3.9 MJ/m
Stored energy density	0.28 J/mm^3

The tape is 12 mm wide and 110 mm thick (Fig. 1). The stainless steel metal-insulator 50 mm thick was introduced for protection reasons[23]. In Table I, the achieved design parameters of the four-layers cosθ dipole are listed. The bore field value has been selected to reduce the collider length, while the temperature margin has been set from the analytical estimates. The blocks are arranged in a 3-4-2-2 layout, featuring the outer layers closer to the midplane to be more efficient in increasing the bore field. The other parameters were then optimized to meet both margin and cost constraints.

III. BRANDT MODEL AND T-A FORMULATION FOR NON-UNIFORM CURRENT CALCULATION

Even tough HTS material presents many advantages w.r.t. LTS in terms of critical surface, REBCO tapes are generally more expensive, and the quench protection is more challenging due to the higher heat capacity of the material. Moreover, the large width of the tapes combined with their non-transposed arrangement within the cables results in significant magnetization (produced by the non-uniform screening currents), which in turn causes considerable hysteretic losses, degrades the bore field uniformity, and generates additional stress inside the coils. To compute the non-uniform current distribution in the 16 T cosθ dipole, a code was developed in MATLAB to apply the Brandt model within the cross-section of each tape. Developed by Brandt and Indenbom (1993), this model describes how the *sheet current* J(A/mm) — the current density integrated over the tape thickness — distributes in a REBCO tape subjected to a uniform perpendicular field $B_\perp$. To adapt the field uniformity assumption of the model to the cosθ magnet study, the mean perpendicular field along each tape is considered. In addition, convergence algorithms account for mutual tape interactions. This code was validated by results obtained from the T-A formulation, a numerical method implemented in COMSOL. The analytical approach of the Brandt model makes the MATLAB code much faster than the T-A formulation (see Sec.IV-B). However, two are the main limits that characterize the analytical tool from the numerical one. Indeed, the former cannot simulate (at least for now) phenomena that are:

1) linked to the ferromagnetic behaviour of the materials (that inevitably arise in presence of an iron yoke around the coils). It means that for the dipole magnet here studied, numerical methods remain essential to evaluate the iron magnetization impact on the design performances.
2) time dependent (e.g. the hysteretic behavior of persistent currents inside the REBCO tapes). Thus, the analytical model can be used only to simulate the first energization of the magnet. Anyway, for steady state magnets (like in this case), this second limit is not so significant.

IV. ELECTROMAGNETIC ANALYSIS

A. Uniform Current

As a preliminary step, the numerical tool ROXIE[24] - limitated to simulating only uniform current distribution inside the conductor - was used to estimate how much the coils and the iron yoke contribute to the bore field and to the field quality. This analysis assessed that:

- with a cylindrical shaped iron yoke 350 mm thick, the coil alone must generate about 14 T;
- since the iron yoke saturates almost completely, it does not affect the field quality significantly.

This second aspect is very important, because it means that - in first approximation - the effects of current distribution on field quality could be studied without the necessity of simulating the iron yoke, enabling the analytical model to obtain useful results for this design study. To evaluate the effects of non-uniform current on field quality (without the iron yoke), the magnet geometry was imported in MATLAB. Before fully exploiting the analytical code potential for simulating screening currents, an initial validation was carried out by assuming a uniform current distribution and comparing the results with those obtained from ROXIE without the yoke.

Fig. 2 shows that the electromagnetic results in absence of iron obtained by the two software are compatible with a relative error of 0.7% related to the field intensity (the difference in the maximum temperature margin is due to the sharp growth of the critical current when the field is quite parallel to the tape). A minimum local temperature margin of 6 K was obtained (with the term *local* we refer that it is not averaged on the tape cross section; the minimum averaged temperature margin is 10 K and considers that the current can redistribute inside the tape avoiding the most critical point to quench) This margin will be obviously reduced with the yoke insertion; for this reason, a new simulation was performed with ROXIE, including the iron yoke and always considering uniform current in order to estimate the margin in the worst case. The results assured that the requirement of a minimum T_{marg} of at least 2.5 K was met. In Table II, the field quality comparison between ROXIE and the analytical code is reported. The sextupole component in the case of uniform current is high since the magnet geometry has

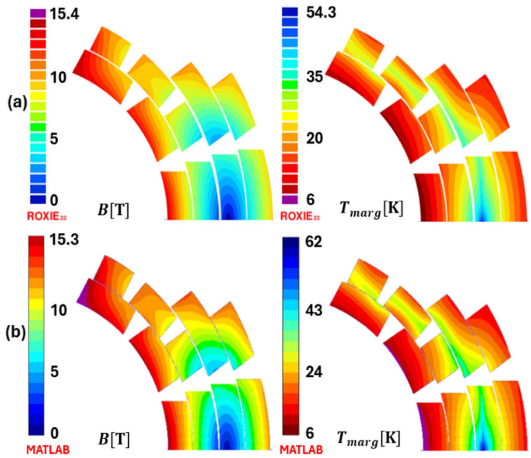

Fig. 2. Electromagnetic results in absence of the iron yoke. (a) field and temperature margin map in ROXIE, (b) field and temperature margin map in MATLAB.

TABLE II
FIELD QUALITY COMPARISON (NO IRON)

Harmonic	ROXIE	MATLAB
b_3	13.3	11.7
b_5	-0.1	-0.1
b_7	0.1	0.1

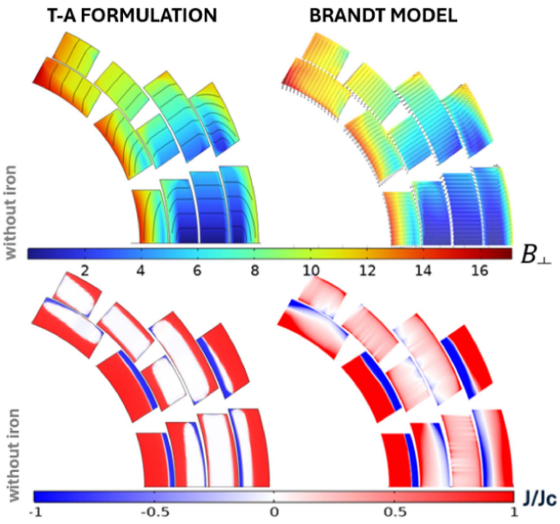

Fig. 3. Field map comparison (top). Current distribution comparison (bottom): positive current outgoing in red, negative current in blue.

been conceived for exploiting the magnetization coming from the screening current effect as field quality corrector.

B. Non-Uniform Current

The code was then compared with the T-A formulation. As expressed in Sec.III, both the approaches account for a non-uniform current distribution. The comparison of the field map and the current distribution of the two models (no yoke) is presented in Fig. 3. Hysteretic losses were also computed and

TABLE III
FIELD QUALITY AND LOSSES COMPARISON (NO IRON)

Harmonic	COMSOL	MATLAB
b_3	5.2	5
b_5	-5.5	0.1
b_7	-2.8	0.1
Q_{hyst}	22.5 kJ/m	22 kJ/m
t	140 min	5 min

Harmonic	Value
b_3	4.2
b_5	-5.5
b_7	-2.9
b_9	-2.9
b_{11}	-2.1

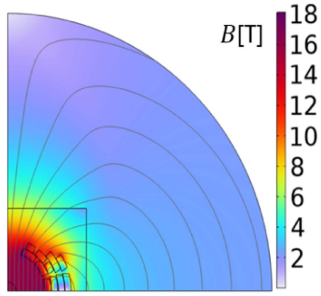

Fig. 4. Field quality considering non-uniform current and the iron yoke effect (left). Coils and iron yoke field map considering non-uniform current (right).

compared. The formula giving their value is:

$$P_{hyst} = M \cdot \frac{dB}{dt} \tag{1}$$

where M(A/m) is the magnetization produced exclusively by shielding currents. Table III shows the results obtained. It must be noted that the sextupole component is reduced by the screening currents. The proximity between the hysteretic losses values integrated over time calculated by the two methods (considering a time of charge of 20 minutes) reflects the similarity in current distribution (Fig. 3, bottom), since the calculation strictly depends on it. Given that the magnet works in steady state and so can tolerate a longer ramp time, the hysteretic power can be easier managed by adjusting the cooling power accordingly. The computational time t of the analytical code for the electromagnetic analysis is 28 times lower than the numerical code.

The results discussed so far - useful to validate the analytical code implementing the Brandt model - do not consider the iron yoke contribution, since, as said in Sec. III, the code cannot study non-linear phenomena. So, once the validation with non-uniform current was also performed, the design study continued in COMSOL with the insertion of the iron yoke inside the geometrical model that will result in Fig. 4. For the reasons explained in Sec. IV-A, the yoke does not change appreciably the field quality, and it is clear also that, since the required temperature margin of 2.5 K is already guaranteed considering uniform current, it remains valid with the non-uniform current assumption, due to field attenuation caused by the screening effect.

V. MECHANICAL ANALYSIS

The screening currents also have an impact on the mechanical design. To assess their effect, a mechanical analysis was carried out in COMSOL under the following assumptions:

- the four layers were considered as bonded together;

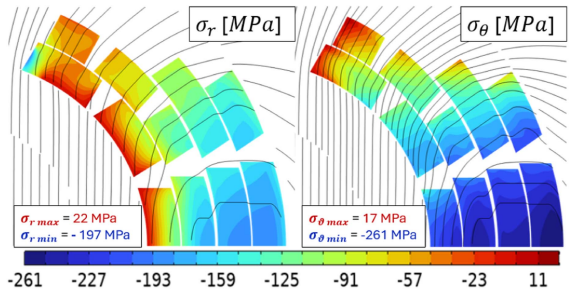

Fig. 5. Radial (left) and azimuthal (right) stress map.

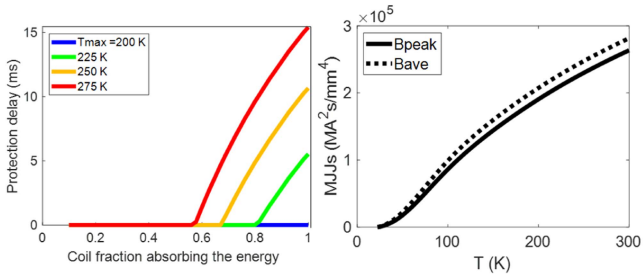

Fig. 6. Maximum temperature depending on coil fraction absorbing the energy and protection delay (left). Maximum temperature depending on the quench integral (right). Solid line considers the peak field B_{peak} in the coil; dotted line considers the average field inside the cable where B_{peak} is reached.

- the collar surrounding the magnet was modeled as infinitely rigid;
- the contact between the collar and the coil layers was assumed to be frictionless;
- the Young's modulus of the coil layers, taken as 174 GPa[25], was computed assuming a homogeneous material;
- the wedges were assumed to be made of copper.

Fig. 5 shows the radial and the azimuthal stress produced by the Lorentz forces. The screening currents produce additional stress to the coils, threatening their degradation. Considering the radial and azimuthal stress limits of 100 MPa and 400 MPa[25], further study is needed to reduce the radial stress inside the coils.

VI. Quench Protection Analysis

One of the main challenges in designing an HTS magnet is the quench protection. In this study, an analytical calculation was performed, providing several useful insights summarized in Fig. 6. A further calculation enabled us to know the maximum admitted stored energy depending on the copper current density J_{Cu}. From the analysis, it was found that with a stored energy density of 0.28 J/mm^3, a $J_{Cu} = 1897\ A/mm^2$ is below the design target limits thereby ensuring compliance with the protection study constraints using conventional quench protection methods.

VII. Cost Model

The model[26] used to evaluate the total cost of the magnet takes LHC dipole as a benchmark[27], [28], and considers three different contributions:

TABLE IV
Density and Cost Per Kilo of Tape and Stabilizer

Parameters and Results	Value
REBCO tape density	7800 kg/m^3
Stainless Steel density	7800 kg/m^3
REBCO tape cost (per kilo)	2671 €/kg
Stainless Steel tape cost (per kilo)	10 €/kg

TABLE V
Cost Contributions and Total Amount

Magnet Section	Cost Breakdown	Value
Coil	Material (C_{SC} +C_{SS}) + Manufacturing	236.2 k€/m
Cold Mass	Material + Manufacturing	74.4 k€/m
Cryogenics	/	8 k€/m
Total	/	**318.6 k€/m**

- cost of the coil material and the manufacturing;
- cost of the cold mass material and the manufacturing;
- cost of the cryogenics.

The cost of the coil material obviously depends on the density and cost per kilo of the different components of the cable shown in Table IV .

Assuming an aspirational tape cost of one third[29] of the actual one, and considering a 8.272 km tape length per meter of coil, the cost values are those shown in table V.

C_{SC} and C_{SS} are respectively the total cost of the superconductor tapes and the total cost of the stainless steel stabilizer inside the cables. The cold mass material cost was obtained by considering its cost in the LHC dipoles and scaling it according to the bore field value ratio $B_{MuCol}/B_{LHC} = 16\ \mathrm{T}/8.33\ \mathrm{T}$. Finally, the cryogenic cost is assumed to be identical to that of the LHC dipoles[30].

VIII. Conclusion

The conceptual design of the cosθ dipole magnet for the Muon Collider ring was performed accounting for the screening currents effect, also trying to obtain benefits from it. The electromagnetic analysis confirmed that all the main requirements are satisfied: bore field of 16 T, temperature margin of 2.5 K, and acceptable field quality. The preliminary mechanical study showed that further work is needed to reduce the maximum radial stress compression of almost 100 MPa. The constraints identified in the quench protection study conducted so far have been satisfied. The total cost of the magnet is much lower than the maximum cost limit, giving space for significant improvements for the next design optimizations. The design study presented in this paper gave also the opportunity of evaluating the accuracy of the analytical code implementing the Brandt model, comparing its results with those obtained by ROXIE and COMSOL. The huge reduction in computational time between the analytical and the numerical simulations was also shown.

Acknowledgment

The authors thank the PNRR-IRIS Project of INFN funded by the Italian Ministry of Research for the financial support. These authors performed this work on behalf of the IMCC.

REFERENCES

[1] C. Accettura et al., "Towards a muon collider," *Eur. Phys. J. C*, vol. 83, no. 9, pp. 1–110, 2023.

[2] D. Schulte, "Jacow: The international muon collider collaboration," *JACoW IPAC*, vol. 2021, pp. 3792–3795, 2021.

[3] D. Stratakis et al., "A muon collider facility for physics discovery," 2022, doi: 10.48550/arXiv.2203.08033.

[4] C. Aime et al., "Muon collider physics summary," 2022, doi: 10.48550/arXiv.2203.07256.

[5] C. Adolphsen et al., "European strategy for particle physics–accelerator R&D roadmap," 2022, *arXiv:2201.07895*.

[6] M. Boscolo et al., "The future prospects of Muon colliders and neutrino factories," *Rev. Accel. Sci. Technol.*, vol. 10, no. 01, pp. 189–214, 2019.

[7] L. Bottura et al., "Magnets for a Muon collider—Needs and plans," *IEEE Trans. Appl. Supercond.*, vol. 34, no. 5, Aug. 2024, Art. no. 4005708.

[8] L. Bottura et al., "A work proposal for a collaborative study of magnet technology for a future Muon collider," 2022, *arXiv:2203.13998*.

[9] B. Caiffi et al., "Challenges and perspectives of the superconducting magnets for the Muon collider storage ring," *IEEE Trans. Appl. Supercond.*, vol. 35, no. 5, Aug. 2025, Art. no. 4002007.

[10] B. Caiffi et al., "Updates on the conceptual design study of the magnets for the Muon collider storage ring," *IEEE Trans. Appl. Supercond.*, vol. 36, no. 3, May 2026, Art. no. 4001505, doi: 10.1109/TASC.2025.3628590.

[11] MATLAB, Version R2023b, The MathWorks, Inc., Natick, Massachusetts, United States, 2023 [Online]. Available: https://www.mathworks.com/products/matlab.html

[12] E. H. Brandt and M. Indenbom, "Type-II-superconductor strip with current in a perpendicular magnetic field," *Phys. Rev. B*, vol. 48, no. 17, 1993, Art. no. 12893.

[13] COMSOL Multiphysics, Version 6.3, COMSOL AB, Stockholm, Sweden, 2024. [Online]. Available: https://www.comsol.com

[14] E. Berrospe-Juarez et al., "Real-time simulation of large-scale HTS systems: Multi-scale and homogeneous models using the T–A formulation," *Supercond. Sci. Technol.*, vol. 32, no. 6, 2019, Art. no. 065003.

[15] D. Novelli et al., "Analytical and numerical study of superconducting dipole and quadrupole performance limits for a Muon collider," *IEEE Trans. Appl. Supercond.*, vol. 35, no. 5, Aug. 2025, Art. no. 4000205.

[16] D. Novelli et al., "Analytical evaluation of dipole performance limits for a Muon collider," *IEEE Trans. Appl. Supercond.*, vol. 34, no. 5, Aug. 2024, Art. no. 4002405.

[17] F. Levi et al., "Magnetic and mechanical design of the large aperture HTS superconducting dipoles for the accelerator ring of the Muon collider," *IEEE Trans. Appl. Supercond.*, vol. 35, no. 5, Aug. 2025, Art. no. 4000905.

[18] P. B. de Sousa et al., "Muon collider magnet technology options internal review-cooling," in *Proc. IMCC Annu. Meeting*, 2023, pp. 19–22.

[19] F. Mariani et al., "Preliminary electromagnetic and mechanical design of a cosθ dipole for the Muon collider study," *IEEE Trans. Appl. Supercond.*, vol. 35, no. 5, Aug. 2025, Art. no. 4000805.

[20] L. Alfonso et al., "Preliminary design of a block-coil magnet for the Muon collider ring," *IEEE Trans. Appl. Supercond.*, vol. 35, no. 5, Aug. 2025, Art. no. 4000405.

[21] L. Alfonso et al., "Updates on the preliminary electromagnetic and mechanical design of the block-coil dipole for the Muon collider ring," unpublished.

[22] Fujikura HTS tape online catalogue. 2024. [Online]. Available: https://www.fujikura.co.uk/netalogue/pdfs/Fujikura%20Superconductor%20Guide.pdf

[23] T. Salmi et al., "Analytical estimation of quench protection limits in insulated, non-insulated, and metal-insulated ReBCO accelerator dipoles and quadrupoles," *IEEE Trans. Appl. Supercond.*, vol. 35, no. 5, Aug. 2025, Art. no. 4604705.

[24] ROXIE - Rotationally Symmetric Magnetostatic and E-Field Calculations, CERN, Geneva, Switzerland, 2025, Sviluppato dal Superconducting Magnet Group (TE-MSC-MDT) del CERN. [Online]. Available: https://cern.ch/roxie

[25] C. Barth et al., "Electro-mechanical properties of REBCO coated conductors from various industrial manufacturers at 77 k., self-field and 4.2 k, 19 t," *Superconductor Sci. Technol.*, vol. 28, no. 4, 2015, Art. no. 045011.

[26] L. Bottura and B. Bordini, "HTS potential and needs for future accelerator magnets," 2025, *arXiv:2503.23048*.

[27] D. Schoerling et al., "Considerations on a cost model for high-field dipole arc magnets for FCC," *IEEE Trans. Appl. Supercond.*, vol. 27, no. 4, Jun. 2017, Art. no. 4003105.

[28] L. Rossi, "Manufacturing and testing of accelerator superconducting magnets," 2015, *arXiv:1501.07164*.

[29] A. Ballarino and L. Bottura, "Targets for R&D on Nb_3Sn conductor for high energy physics," *IEEE Trans. Appl. Supercond.*, vol. 25, no. 3, Jun. 2015, Art. no. 6000906.

[30] A. Poncet and V. Parma, "Series-produced helium II cryostats for the LHC magnets: Technical choices, industrialisation, costs," in *Proc. AIP Conf. Proc.*, 2008, vol. 985, no. 1, pp. 739–746.